Journal of Dental Sciences 21 (2026) 484–493

Available online at www.sciencedirect.com

ScienceDirect

journal homepage: www.e-jds.com

Original Article

Biofunctionalized 3D-printed gelatin-alginate scaffolds with arginine-glycine-aspartic acid (RGD) peptides for enhanced *in vitro* osteogenesis

Ting-Yi Renn [a,1], You-Ru Ma [a,1], Chia-Chen Hsu [a,b], Eisner Salamanca [a], Hiroshi Egusa [c,d], Ying-Sui Sun [e], Chun-Pin Lin [f,g*], Wei-Jen Chang [a,b**]

[a] *School of Dentistry, College of Oral Medicine, Taipei Medical University, Taipei, Taiwan*
[b] *Dental Department, Shuang-Ho Hospital, Taipei Medical University, New Taipei City, Taiwan*
[c] *Center for Advanced Stem Cell and Regenerative Research, Tohoku University Graduate School of Dentistry, Miyagi, Japan*
[d] *Division of Molecular & Regenerative Prosthodontics, Tohoku University Graduate School of Dentistry, Miyagi, Japan*
[e] *School of Dental Technology, College of Oral Medicine, Taipei Medical University, Taipei, Taiwan*
[f] *Department of Dentistry, National Taiwan University Hospital, Taipei, Taiwan*
[g] *Graduate Institute of Clinical Dentistry, School of Dentistry, National Taiwan University, Taipei, Taiwan*

Received 22 October 2025; Final revision received 23 October 2025
Available online 6 November 2025

KEYWORDS
3D printing;
Hydrogel;
Bone regeneration;
Gelatin-alginate;
Arginylglycylaspartic acid (RGD)

Abstract *Background/purpose:* Alveolar bone defects are difficult to treat due to ongoing resorption and limitations of conventional grafts. Tissue engineering strategies, particularly 3D hydrogel-based scaffolds, offer promising alternatives by mimicking the extracellular matrix and supporting cell-driven regeneration. This study aimed to incorporating arginine-glycine-aspartic acid (RGD) peptides into 3D-printed gelatin-alginate hydrogels to enhances their bioactivity and osteogenic potential for effective alveolar bone repair.
Materials and methods: The physical characterization of RGD peptides-grafted 3D-printed gelatin-alginate scaffolds was conducted using morphological observation, elemental

* Corresponding author. School of Dentistry, National Taiwan University and National Taiwan University Hospital, No. 1 Chang-Te Street, Taipei, 100229, Taiwan.
** Corresponding author. School of Dentistry, College of Oral Medicine, Taipei Medical University, No. 250, Wu-Hsing Street, Xinyi District, Taipei city, 110, Taiwan.
E-mail addresses: pinlin@ntu.edu.tw (C.-P. Lin), cweijen1@tmu.edu.tw (W.-J. Chang).
[1] Ting-Yi Renn and You-Ru Ma are designated as co-first authours.

https://doi.org/10.1016/j.jds.2025.10.030

composition analysis, Fourier-transform infrared spectroscopy (FTIR), and assessments of swelling and degradation behavior. Biological performance was examined *in vitro* through cell adhesion, proliferation, differentiation (proven by alkaline phosphatase activity), and mineralization (proven by Alizarin red S staining) using MG-63 osteoblastic-like cells.
Results: RGD peptides-grafted 3D-printed gelatin-alginate scaffolds exhibited a porous architecture. Elemental and FTIR analyses confirmed successful peptide incorporation through elevated nitrogen and oxygen content, along with amide and C—H stretching bands. The scaffolds showed stable swelling, reduced degradation, and significantly enhanced MG-63 cell adhesion, proliferation, ALP activity, and mineralization, particularly in the 0.5 mg/mL RGD peptides-grafted group.
Conclusion: RGD peptides modification significantly enhances the structural and biological performance of 3D gelatin-alginate scaffolds, reinforcing their potential as effective materials for alveolar bone regeneration.

Introduction

Alveolar bone defects involve the degradation or loss of the bone that supports teeth, often resulting from periodontitis, cavities, trauma, developmental issues, or tooth removal.[1] These defects are widespread, particularly in older populations, and frequently lead to ongoing alveolar bone resorption, which affects oral functionality, appearance, and prosthetic treatments.[2] Socket preservation, also known as alveolar bone preservation, is a preventive surgical method designed to reduce bone loss after tooth extraction. This technique includes filling the socket with graft materials like autografts, allografts, xenografts, or synthetic alternatives, often used alongside barrier membranes.[3,4] However, the long-term success of these materials is limited due to challenges such as inadequate resorption control, immune responses, and the development of non-vital, scar-like bone tissue. Furthermore, complex defect shapes, poor bone quality, and infection risks add to the treatment difficulties.[5,6] Consequently, achieving reliable bone regeneration is a crucial goal in contemporary dentistry, vital for preserving facial structure, ensuring implant success, and restoring oral function. These clinical challenges underscore the necessity for advanced biomaterials and regenerative approaches to improve the results of alveolar bone preservation and repair.[3]

Tissue engineering and regenerative medicine (TERM) have become promising alternatives to traditional bone grafting methods, overcoming the drawbacks of autografts, allografts, and synthetic implants.[7,8] These strategies involve the integration of scaffolds, cells, and growth factors—or sometimes just scaffolds—to develop constructs that can promote tissue repair and regeneration.[9] Scaffolding materials are crucial as they create a microenvironment that facilitates cell adhesion, growth, and differentiation. An ideal scaffold should replicate the extracellular matrix (ECM), have appropriate physicochemical characteristics, and be both biocompatible and biodegradable. Consequently, the creation of advanced biomimetic scaffolds that can regulate essential cellular activities and deliver bioactive signals which are vital for improving targeted bone regeneration.[10] Among tissue engineering approaches, hydrogels have emerged as highly promising scaffolding materials due to their biocompatibility, biodegradability, and ability to mimic the ECM.[11] Their tunable physical and biological properties—such as cross-linking density, degradation rate, and cargo release—allow customization for alveolar bone regeneration. Hydrogels can encapsulate cells and bioactive molecules while supporting cell adhesion, proliferation, and differentiation in a moist, 3D environment. Additionally, their injectability and integration with surrounding tissues reduce the need for secondary surgery, positioning them as ideal candidates for addressing the challenges of alveolar bone defect repair.[12,13]

Meanwhile, the advancement of three-dimensional (3D) printing technology has revolutionized the fabrication of biomedical devices and customized tissue constructs. This layer-by-layer production approach enables the assembly of various biomaterials into patient-specific, multiphasic structures, significantly enhancing the precision and adaptability of scaffold design.[14] The primary conduit of 3D bioprinting is the bio-ink. Using hydrogel-based bio-inks, 3D bioprinting allows for spatial control over scaffold architecture, enabling the creation of complex structures that closely mimic native tissue geometry.[15] Two widely studied hydrogel materials for bio-ink are gelatin and alginate. Gelatin, a non-immunogenic collagen derivative widely used in tissue engineering, forms hydrogels with collagen-like properties but suffers from poor mechanical strength and rapid degradation at body temperature, requiring chemical crosslinking—often with toxic agents—which limits its application in cell-laden constructs.[16] GelMA, a photocrosslinkable derivative of gelatin,[17] retains cell-adhesive motifs and offers good biocompatibility.[18] However, it suffers from inherent limitations, such as low mechanical stiffness and limited osteoinductive capacity, especially when applied alone in load-bearing environments.[19] Alginate, derived from brown seaweed, provides

better structural integrity and printability but lacks integrin-binding sites, resulting in poor cell adhesion and bioactivity.[20] Therefore, researchers are increasingly seeking ways to combine or functionalize these hydrogels to improve their performance in bone tissue engineering.

To enhance the biological activity of hydrogel-based scaffolds, one promising strategy is the incorporation of cell-adhesive peptides, particularly the arginine-glycine-aspartic acid (RGD) motif. RGD peptides are well-known for their ability to bind to integrin receptors on cell surfaces, thereby promoting cell adhesion, proliferation, and differentiation.[21] When introduced into hydrogel networks such as alginate or GelMA, RGD peptides can compensate for the material's inherent limitations in bioactivity, effectively facilitating improved cell—material interactions.[22,23] This is especially important for osteogenic applications, as enhanced adhesion and spreading of osteoblasts or stem cells within the scaffold environment are critical for initiating bone tissue formation. Recent studies have demonstrated that RGD-functionalized hydrogels can significantly upregulate osteogenic markers and support better mineralization *in vitro* and *in vivo*.[21] Therefore, the combination of RGD peptides with 3D-printed gelatin- and alginate-based scaffolds holds great potential for precisely engineered bone graft substitutes that offer both mechanical stability and biological functionality.

This study aimed to develop a 3D bio-printed hydrogel scaffold composed of RGD peptides-grafted gelatin- and alginate-based mixture for alveolar bone preservation. The research focused on evaluating the physical, chemical, and biological properties of hybrid hydrogel, as well as its ability to support osteogenic differentiation and promote bone tissue regeneration. By incorporating bioactive RGD peptides into a biocompatible and printable gelatin-alginate hydrogel, this study sought to overcome the limitations of current materials and provide a novel approach for periodontal and alveolar bone regeneration.

Materials and methods

Preparation of printing hydrogel

To prepare the homogeneous printing-ink, gelatin powder (15 % w/v) (type B, Sigma—Aldrich, St. Louis, MO, USA) was first dissolved in phosphate-buffered saline (PBS) and stirred at 37 °C until a clear homogenous gelatin solution was obtained. Sodium alginate powder (1 % w/v) (Sigma—Aldrich) was added to the gelatin solution to obtain gelatin-alginate hydrogel mixtures. The resulting hydrogel mixture was then ready for 3D printing.

Fabrication of arginine-glycine-aspartic acid (RGD) peptides-grafted gelatin-alginate scaffolds

Before printing the scaffolds in a bioprinter, the hydrogel mixture was maintained at 37 °C. For scaffold fabrication, the prepared hydrogel mixture was loaded into a syringe and transferred into the printing cartridge equipped with a 22G nozzle on a BioX bioprinter (Cellink, Boston, MA, USA). A 10 cm culture dish was placed beneath the pneumatic printhead, and after optimizing the printing position and parameters, the bioprinting process was initiated. Three-dimensional cylindrical scaffolds (10 mm × 10 mm × 1 mm) with honeycomb infill pattern were printed at a speed of 3 mm/s under an extrusion pressure ranging from 30 to 90 kPa. The print bed and nozzle temperature were fixed at 15 °C and 37 °C, respectively. Following printing, the constructs were crosslinked in a 100 mM $CaCl_2$ solution for 10 min, then washed three times with PBS to remove residual $CaCl_2$ and ensure structural integrity and stability. RGD peptides were then grafted onto the hydrogel mixture at concentrations of 0.25 mg/mL and 0.5 mg/mL using an immersion grafting method for 24 h to enhance bioactivity.

Physical and chemical characterization of arginine-glycine-aspartic acid (RGD) peptides-grafted gelatin-alginate scaffolds

Scaffold samples were fixed by 2 % glutaraldehyde for an hour, then washed in saline and then freeze dried with an ice condenser temperature of −55 °C for 24 h. Each sample was coated with 10 nm layer of gold and then the surface morphology was collected by scanning electron microscope (SEM; Hitachi, Ltd., Tokyo, Japan). Surface elemental analysis was conducted by energy-dispersive X-ray spectroscopy (EDS; Bruker Quantax, Germany).

To characterize the chemical composition and functional group modifications of RGD peptides-grafted gelatin-alginate scaffolds, Fourier-transform infrared spectroscopy (FTIR; Thermo Scientific, Waltham, MA, USA) was performed. The spectra of samples were recorded in the range of 4000—650 cm^{-1} with 16 scans with a resolution of 0.482 cm^{-1}.

The swelling and degradation properties of scaffold samples were evaluated by weighing method at different time points after immersion in cell culture medium at 37 °C for 6 h. The swelling and degradation ratio of the samples were calculated according to the following formulation:

$$\text{Swelling (w\%) or Degradation (w\%)} = \frac{Wt\text{-}Wi}{Wi} \times 100$$

where positive values are considered as swelling and negative values are considered as degradation. *Wi* is the initial weight, and *Wt* is the weight at the predetermined time points.

Biological responses of arginine-glycine-aspartic acid (RGD) peptides-grafted gelatin-alginate scaffolds

The human immortalized osteoblastic cell line MG-63 obtained from the Bioresource Collection and Research Center (BCRC 60279, BCRC, Hsinchu City, Taiwan) was used in this study. The cells were cultured in Minimum Essential Medium Eagle (MEM; Corning, Corning, NY, USA) supplemented with 10 % fetal bovine serum (FBS; Avantor, Radnor, PA, USA) and 1 % penicillin streptomycin (P/S; Gibco, Grand Island, NY, USA) under humidified condition with 5 % CO_2 at 37 °C.

Cell adhesion observation by immunofluorescent microscopy

After 24 and 48 h of cell seeding, the specimens were washed with PBS and fixed with 4 % paraformaldehyde for 30 min. The cells were then permeabilized using 0.1 % Triton X-100 for 15 min, followed by blocking with 2 % bovine serum albumin (BSA) for 1 h to prevent nonspecific binding. The specimens were stained for actin with FITC-phalloidin (AB176753, Abcam, Cambridge, UK) for 1 h at room temperature, and nuclei were subsequently counterstained with DAPI (4',6-diamidino-2-phenylindole, dilactate; D9542 Sigma–Aldrich Chemie GmbH, Deisenhofen, Germany) for 15 min at room temperature. The cell adhesion was observed using a fluorescence microscope (Nikon Corporation, Tokyo, Japan).

Cell proliferation assessment by Alamar blue assay

Cell proliferation on the scaffolds was evaluated using the Alamar blue assay (BUF012B; AbD Serotec, Kidlington, UK), which quantifies cellular metabolic activity as an indicator of cell viability and growth. MG-63 osteoblastic-like cells were seeded at density of 5×10^4 onto scaffolds. The assay was conducted at various time points 1, 3, 5, and 7 days after seeding to assess cell proliferation. The optical density of Alamar blue was obtained by measuring changes of absorbance at 570 nm and 600 nm using a spectrophotometer.

Cell differentiation ability by alkaline phosphatase assay

The activity of alkaline phosphatase (ALP), a key indicator of osteoblastic differentiation and function, was determined using the Abcam ALP Assay Kit (ab83369, Abcam, UK). Briefly, MG-63 cells were seeded onto the scaffolds at a density of 5×10^4 cells/cm^2, and the supernatants were collected for ALP assay at 7 and 14 days. The ALP activity was quantified by measuring the absorbance at 405 nm using a spectrophotometer.

Cell mineralization ability by Alizarin red S (ARS) staining

Mineralization activity was evaluated at 7 and 14 days after incubation on the scaffolds. The cells were fixed with 4 % paraformaldehyde for 30 min, washed with PBS, and subsequently stained with 0.2 % Alizarin red S solution (Sigma–Aldrich) for 10 min to visualize calcium deposits. To quantify the mineralization, the bound Alizarin red S dye was dissolved using 10 % hexadecylpyridinium chloride monohydrate solution, and the absorbance was then measured at 540 nm using a spectrophotometer.

Statistical analysis

The data from the experimental analyses were described using means and standard deviations. All statistical analyses were performed using two-way analysis of variance (ANOVA), and Tukey multiple comparisons test by Prism (v10; GraphPad Software Inc., Boston, MA, USA). Values of $P < 0.05$ were considered statistically significant.

Results

Morphology and element characterization of arginine-glycine-aspartic acid (RGD) peptides-grafted gelatin-alginate scaffolds

Two views of the hydrogel scaffold before and after freeze-drying are shown in Fig. 1A. The left image shows the scaffold in its hydrated state, immediately after 3D printing, while the right image shows the same scaffold following freeze-drying. The overall structure, including its shape and dimensions, is well preserved after drying process. Notably, the scaffold exhibits a regular and interconnected porous architecture, with uniformly distributed pores that remain clearly visible. The optical microscope images (Fig. 1B) show the macroscopic structure within the hydrogel scaffold, a porous structure is revealed with interconnected fiber-like elements.

The surface morphology observed by SEM is shown in Fig. 2A. SEM images showed the presence of fiber-like structures within the scaffold, which are likely resulting from the crosslinking of gelatin. Spherical particles on the surface of gelatin-alginate scaffold are presented, however, these particles reduced within the increase concentrations of RGD peptide modification of scaffold. Compared to the non-modified gelatin-alginate scaffold, the surfaces of 0.5 mg/mL RGD peptides-grafted gelatin-alginate scaffold exhibits more texture and clear pore boundaries. The elemental composition (by weight%) of carbon (C), nitrogen (N), and oxygen (O) of RGD peptides-grafted gelatin-alginate scaffolds was further analyzed with EDS (Fig. 2B). The results demonstrate that increasing RGD concentration in the hydrogel composition leads to a decrease in carbon proportion and a notable increase in both nitrogen and oxygen content, consistent with the introduction of RGD peptides containing nitrogen and oxygen atoms.

Structural characterization of arginine-glycine-aspartic acid (RGD) peptides-grafted gelatin-alginate scaffolds

The chemical composition and functional group modifications analysis of RGD peptides-grafted gelatin-alginate scaffolds are shown in Fig. 3. The results show characteristic absorption peaks of gelatin within the hydrogel scaffold, including the N–H stretching vibration at 3300-3500 cm^{-1}, the amide I band (C=O stretching) at 1650 cm^{-1}, and the amide II band (C–N–H bending) at 1540 cm^{-1}, as well as characteristic peaks of alginate corresponding to COO- stretching and C–O–C stretching vibrations. In RGD peptides-grafted gelatin-alginate scaffold, notable absorption peaks appearing between 2850 and 2950 cm^{-1}, which attributed to C–H stretching vibrations. Peaks at 2846 cm^{-1} and 2915 cm^{-1} in RGD peptides-grafted gelatin-alginate scaffold group originating from $-CH_2-$ and $-CH_3$ groups present in aliphatic side chains of amino acids like arginine and glycine. Within the 1480-1580 cm^{-1} region, both amide I

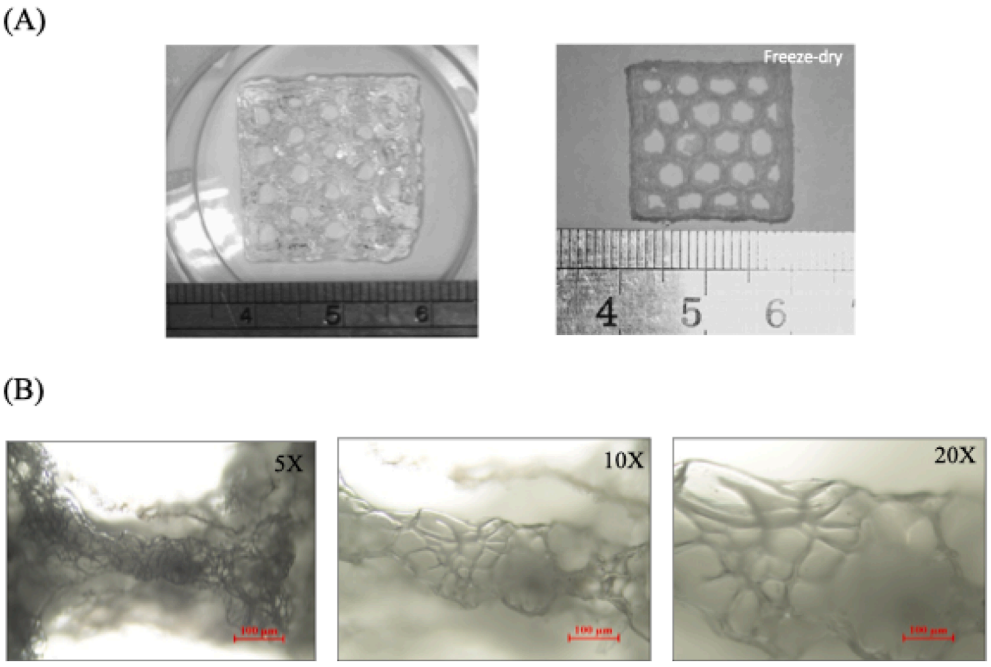

Figure 1 (A) Morphology of 3D-printed gelatin-alginate hydrogel scaffolds before and after freeze-drying. (B) Optical microscopy images of gelatin-alginate scaffolds at different magnifications.

and amid II bands are observed; the amide II band shifts from 1580 in Gel-Alg to 1540 in RGD peptides-grafted gelatin-alginate groups, accompanied by a noticeable increase correlating with higher RGD concentrations.

Swelling and degradation analysis of arginine-glycine-aspartic acid (RGD) peptides-grafted gelatin-alginate scaffolds

Fig. 4 shows the results of swelling and degradation behavior of RGD peptides-grafted gelatin-alginate scaffolds. The gelatin-alginate scaffold showed a progressive and substantial degradation at all observed time points, evidenced by a negative ratio approaching −50 % after 24 h, which then remained steadily. In contrast, both RGD peptides-grafted gelatin-alginate groups exhibited significantly increased swelling ratios that remained relatively stable and positive throughout entire duration. The swelling ratio of the 0.25 mg/mL RGD peptides-grafted gelatin-alginate group peaked at over 30 % within the first 1—8 h and remained elevated up to 30 h, whereas the 0.5 mg/mL RGD peptides-grafted gelatin-alginate group maintained a moderate but consistent swelling of approximately 20 %.

Cell adhesion observation on arginine-glycine-aspartic acid (RGD) peptides-grafted gelatin-alginate scaffolds

The immunofluorescence images (Fig. 5) show the MG-63 cell adhesion and morphology on RGD peptides-grafted gelatin-alginate scaffolds. After cells seeding onto the scaffolds for 6 h, non-adherent cells were observed to remain round in shape across all groups, and actin staining revealed that the cytoskeleton had not spread yet. By 24 h, a significant expansion of the cytoskeletal staining in certain area was observed, indicating that the cytoskeleton had spread and cells had adhered to the scaffold surface. These findings confirm successful cell adhesion to RGD peptides-grafted gelatin-alginate scaffolds with varying concentration of RGD. In addition, MG-63 cells cultured on 0.5 mg/mL RGD peptides-grafted gelatin-alginate scaffold showed a marked increase in cell density and extensive cell spreading.

Cell proliferation ability of MG-63 on arginine-glycine-aspartic acid (RGD) peptides-grafted gelatin-alginate scaffolds

The cell proliferation assessment of MG-63 on RGD peptides-grafted gelatin-alginate scaffolds over a time course of 1, 3, and 5 days are presented in Fig. 6. Over time, all groups exhibited a progressive increase in cell proliferation. However, the gelatin-alginate group showed significantly lower cell proliferation rate than both RGD peptides-grafted gelatin-alginate group at each time point. There's no statistically significant difference between 0.25 mg/mL RGD peptides-grafted and 0.5 mg/mL RGD peptides-grafted groups.

Cell differentiation ability of MG-63 on arginine-glycine-aspartic acid (RGD) peptides-grafted gelatin-alginate scaffolds

ALP activity is a key marker for osteogenic cell differentiation. On both Day 7 and Day 14, the RGD peptides-grafted gelatin-alginate groups exhibited significantly higher ALP activity compared to the control group ($P < 0.001$) (Fig. 7A). Notably, the 0.5 mg/mL RGD peptides-grafted

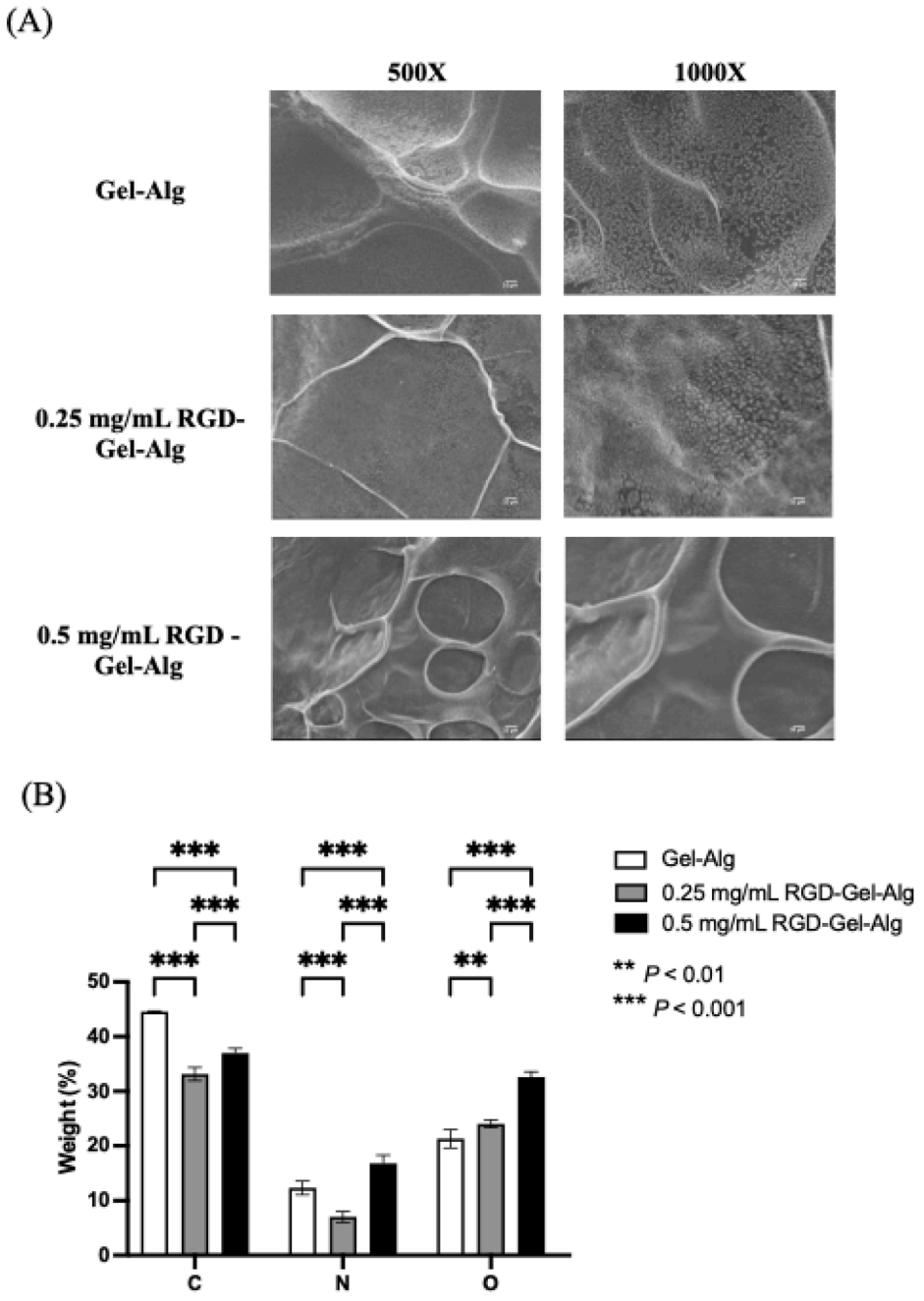

Figure 2 (A) Surface morphology of 3D-printed gelatin-alginate and arginine-glycine-aspartic acid (RGD) peptides-grafted gelatin-alginate scaffolds under scanning electron microscope (SEM). (B) Elemental composition of carbon (C), nitrogen (N), and oxygen (O) in the scaffolds as determined by energy-dispersive X-ray spectroscopy (EDS). Gel-Alg: gelatin-alginate.

gelatin-alginate group showed the highest ALP activity at both time points, with significant increased ($P < 0.05$ on Day 7, $P < 0.001$ on Day 14) than 0.25 mg/mL RGD peptides-grafted gelatin-alginate group.

Cell mineralization ability of MG-63 on arginine-glycine-aspartic acid (RGD) peptides-grafted gelatin-alginate scaffolds

The quantitative assessment of ARS staining is shown in Fig. 7B. The O.D. values of both RGD peptides-grafted groups increased from Day 7 to Day 14, indicating time-dependent progression of cell mineralization with RGD peptides-grafted gelatin-alginate scaffolds. Moreover, the 0.5 mg/mL RGD peptides-grafted gelatin-alginate group showed the higher intensity at both time points, with significant increased ($P < 0.001$) than 0.25 mg/mL RGD peptides-grafted gelatin-alginate group.

Discussion

This study demonstrated that 3D bio-printed gelatin-alginate hydrogel scaffolds composed of RGD peptides-grafted may improve the material stability, and cellular responses

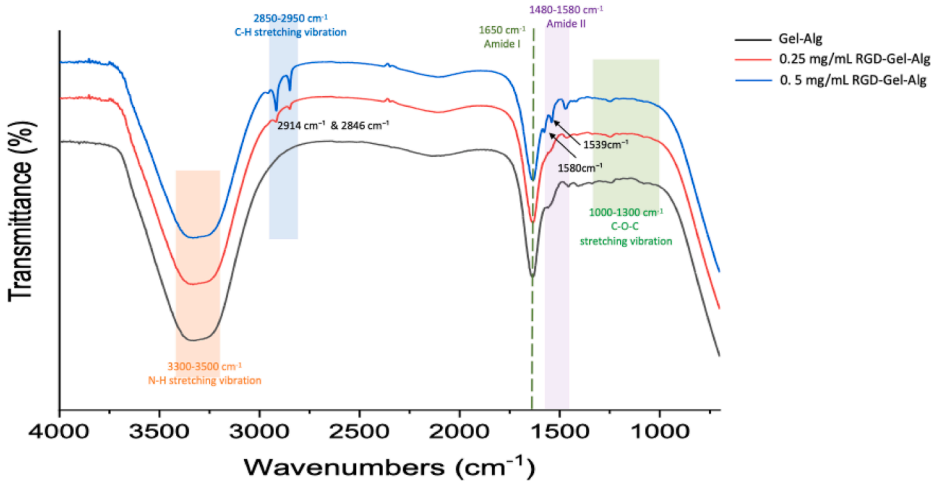

Figure 3 Fourier-transform infrared spectroscopy (FTIR) spectra of gelatin-alginate and arginine-glycine-aspartic acid (RGD) peptides-grafted gelatin-alginate scaffolds. Gel-Alg: gelatin-alginate.

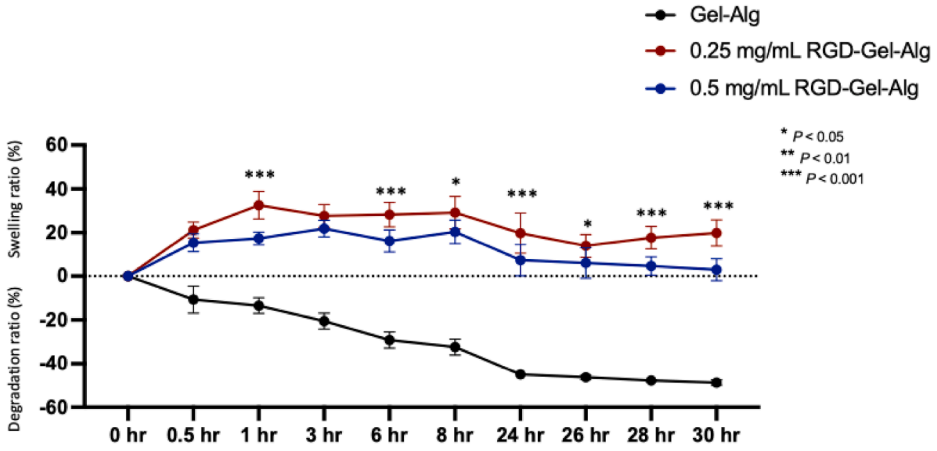

Figure 4 Swelling and degradation ratio of gelatin-alginate and arginine-glycine-aspartic acid (RGD) peptides-grafted gelatin-alginate scaffolds. Gel-Alg: gelatin-alginate.

relevant to alveolar bone tissue engineering. 3D scaffolds offer an exciting possibility to mimic functionality and complexity of native tissues. This result can advance address critical clinical challenges such as the irregularity of defect shapes and the need for reproducible bone regeneration in socket preservation and alveolar bone repair, areas where conventional bone graft materials have shown limited long-term efficacy due to poor integration and variable remodeling capacity.

The freeze-dried 3D RGD peptides-grafted gelatin-alginate scaffolds retained their shape and showed an interconnected porous architecture, similar to previously reported hydrogel designs that optimize nutrient transport and cell migration by maintaining a highly open network structure.[24,25] SEM further confirmed fiber-like surface features of gelatin-alginate and RGD peptides-grafted gelatin-alginate scaffolds. The spherical structures can be observed on the surface of gelatin-alginate samples, these structures result from the formation of polysaccharide polyelectrolyte complexes (PECs) between sodium alginate and gelatin, along with their aggregates.[26] However, these spherical structures decreased with increasing concentrations of RGD peptide modification on the scaffold, which may be attributed to supramolecular interactions promoted by the grafted amino acids, such as hydrogen bonding an van der Waals forces with the hydroxyl and carboxyl groups of alginate. Further EDS analysis confirmed the increased nitrogen and oxygen content in 0.5 mg/mL RGD peptides-grafted gelatin-alginate samples, which is consistent with the incorporation of RGD peptide sequences rich in amino and carboxyl groups. Similar results were observed in the FTIR analysis, which revealed that not only were the typical gelatin and alginate functional groups present, but the RGD peptides-grafted gelatin-alginate scaffold also introduced prominent C—H stretching bands (2915 and 2846 cm^{-1}), along with shifts in the amide II band from 1580 to 1540 cm^{-1}, correlating with higher RGD content. These spectral changes are consistent with previous studies on RGD-functionalized hydrogels, where new amide linkages and side-chain C—H vibrations confirm the integration of biofunctional peptide.[24,27,28] Swelling and degradation data showed that RGD peptides-grafted gelatin-alginate scaffolds maintained stable and positive swelling ratios and resisted progressive hydrogel degradation, unlike

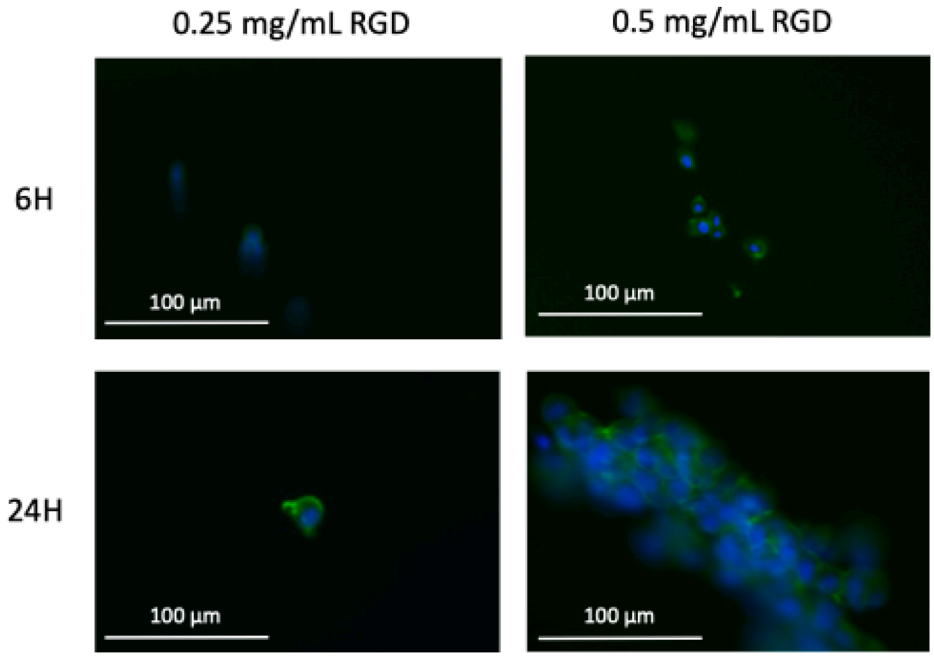

Figure 5 Immunofluorescence images of MG-63 cells seeded on arginine-glycine-aspartic acid (RGD) peptides-grafted gelatin-alginate scaffolds. Blue color indicates cell nuclei (DAPI), and green color indicates the cytoskeleton (actin). (For interpretation of the references to color in this figure legend, the reader is referred to the Web version of this article.)

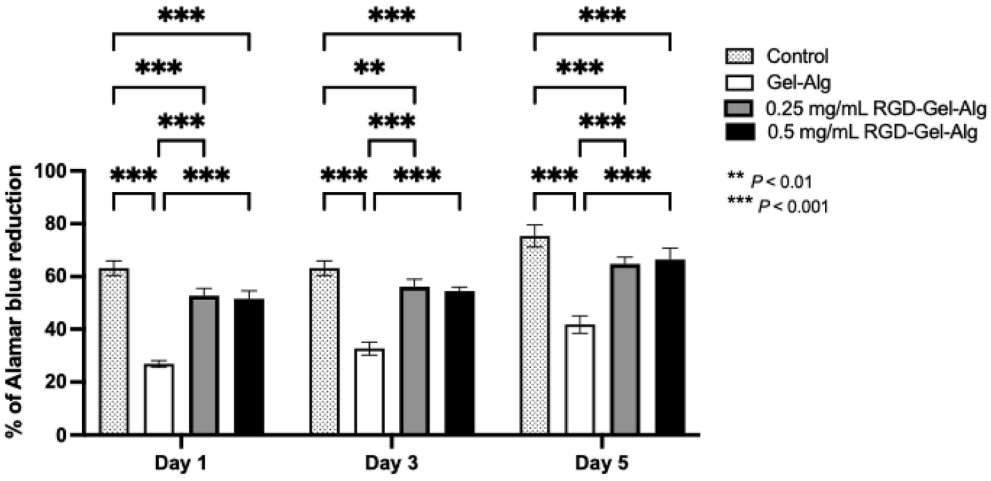

Figure 6 Cell proliferation of MG-63 on arginine-glycine-aspartic acid (RGD) peptides-gaafted gelatin-alginate scaffolds. Gel-Alg: gelatin-alginate.

unmodified gelatin-alginate scaffolds. These findings agree with Cao et al., who reported that RGD incorporation stabilizes hydrogel architecture during *in vitro* culture.[29] The ability to balance swelling with degradation helps scaffold integrity synchronize with natural bone regeneration rates, a key design factor for osteoporotic bone repair.

In our *in vitro* experiments, cell attachment on RGD peptides-grafted gelatin-alginate scaffolds showed better MG-63 cell adhesion and spreading, particularly at 0.5 mg/mL RGD concentration. This phenomenon confirms the ability of RGD grafting help to promote integrin-mediated cell attachment and cytoskeletal organization. These results are supported by findings from Beamish et al., and Yang et al., who demonstrated that RGD modification stimulates integrin activation, initial cell adhesion, and cytoskeletal spreading across various hydrogel matrices.[21,30] Cell proliferation assays confirmed sustained and enhanced growth of MG-63 cells on RGD peptides-grafted gelatin-alginate scaffolds relative to gelatin-alginate. No significant difference was seen between the two RGD concentrations, implying that both levels provide sufficient bioactivity for cell expansion—a finding consistent with prior reports that even low RGD densities can optimize proliferation if distributed uniformly.[31] Elevated ALP activity and mineralization (ARS staining) in RGD peptides-grafted gelatin-alginate scaffolds further demonstrate a dose-dependent

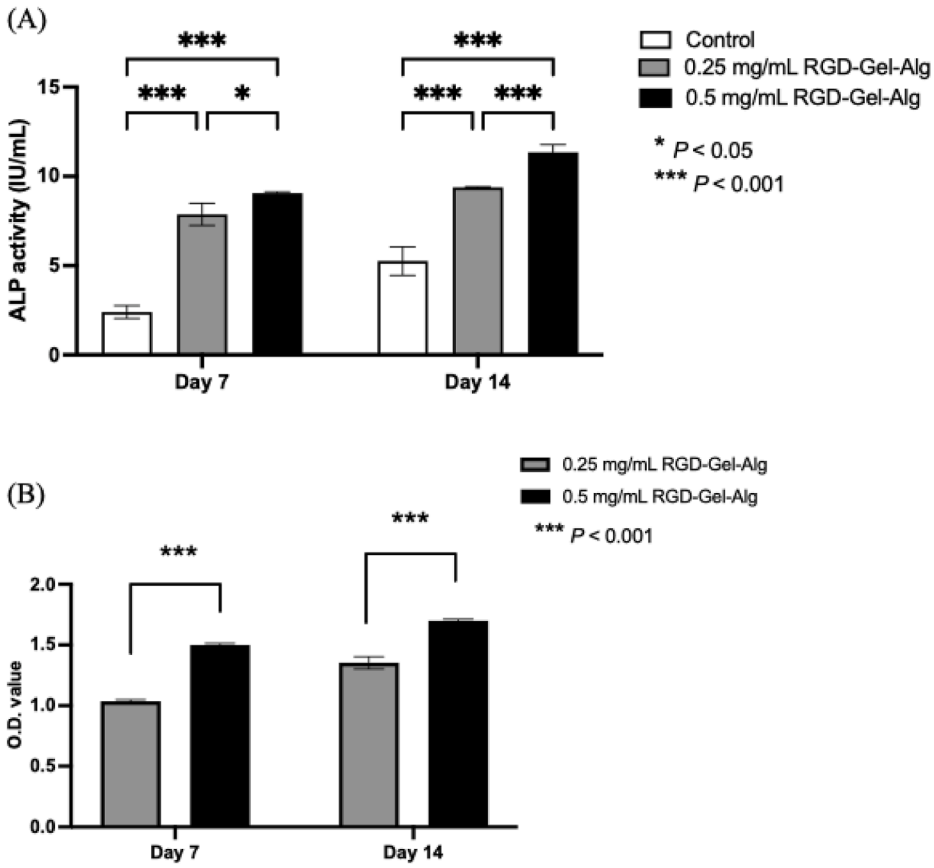

Figure 7 Cell differentiation (A) and mineralization (B) of MG-63 on arginine-glycine-aspartic acid (RGD) peptides-grafted gelatin-alginate scaffolds. ALP: alkaline phosphatase; Gel-Alg: gelatin-alginate.

promotion of osteogenic differentiation and mineralization, aligning with studies that showed improved bone marker expression and calcification in RGD-enriched scaffolds.[32,33] While some reviews suggest that RGD's primary effect is on cell adhesion rather than differentiation,[21,34] our results indicate clear enhancements in both osteogenic commitment and mineral output at higher RGD concentration, likely due to combined effects of improved initial adhesion and microenvironmental signaling.

Taken together, our findings highlight the multifunctionality of RGD peptide modification in natural polymer hydrogel scaffolds - enhancing microstructure, stability, cell adhesion, proliferation, and osteogenic differentiation. These results confirm and expand upon previous conclusions that RGD peptide-modified hydrogels provide a powerful platform for bone regeneration applications.

Declaration of competing interest

The authors have declared that there are no competing interests.

Acknowledgements

This research was funded by the research grants from Taipei Medical University-National Taiwan University Hospital (TMU-NTUH) Joint Research Program [113-TMU-05].

References

1. Collaborators GOD, Bernabe E, Marcenes W, et al. Global, regional, and national levels and trends in burden of oral conditions from 1990 to 2017: a systematic analysis for the global burden of disease 2017 study. *J Dent Sci* 2020;99:362—73.
2. Lantto A, Lundqvist R, Wårdh I. Quality of life related to tooth loss and prosthetic replacements among persons with dependency and functional limitations. *Acta Odontol Scand* 2020;78:173—80.
3. Marian D, Toro G, D'Amico G, et al. Challenges and innovations in alveolar bone regeneration: a narrative review on materials, techniques, clinical outcomes, and future directions. *Medicina* 2024;61:20.
4. Dimova C. Socket preservation procedure after tooth extraction. *Key Eng Mater* 2014;587:325—30.
5. Bannister SR, Powell CA. Foreign body reaction to anorganic bovine bone and autogenous bone with platelet-rich plasma in guided bone regeneration. *J Periodontol* 2008;79:1116—20.
6. Sharma P, Saurav S, Tabassum Z, et al. Applications and interventions of polymers and nanomaterials in alveolar bone regeneration and tooth dentistry. *RSC Adv* 2024;14:36226—45.
7. Esdaille CJ, Washington KS, Laurencin CT. Regenerative engineering: a review of recent advances and future directions. *Regen Med* 2021;16:495—512.
8. Battafarano G, Rossi M, De Martino V, et al. Strategies for bone regeneration: from graft to tissue engineering. *Int J Mol Sci* 2021;22:1128.

9. Tollemar V, Collier ZJ, Mohammed MK, Lee MJ, Ameer GA, Reid RR. Stem cells, growth factors and scaffolds in craniofacial regenerative medicine. *Genes Dis* 2016;3:56—71.
10. Fattahi R, Mohebichamkhorami F, Taghipour N, Keshel SH. The effect of extracellular matrix remodeling on material-based strategies for bone regeneration. *Tissue Cell* 2022;76:101748.
11. Zhong R, Talebian S, Mendes BB, et al. Hydrogels for RNA delivery. *Nat Mater* 2023;22:818—31.
12. Yu Y, Yu T, Wang X, Liu D. Functional hydrogels and their applications in craniomaxillofacial bone regeneration. *Pharmaceutics* 2022;15:150.
13. Xu Z, Wang J, Gao L, Zhang W. Hydrogels in alveolar bone regeneration. *ACS Biomater Sci Eng* 2024;10:7337—51.
14. Hutmacher DW. Scaffold design and fabrication technologies for engineering tissues—state of the art and future perspectives. *J Biomat Sci-Polym E* 2001;12:107—24.
15. Ostrovidov S, Ramalingam M, Bae H, et al. Bioprinting and biomaterials for dental alveolar tissue regeneration. *Front Bioeng Biotechnol* 2023;11:991821.
16. Wang Y, Ma M, Wang J, et al. Development of a photo-crosslinking, biodegradable GelMA/PEGDA hydrogel for guided bone regeneration materials. *Materials (Basel)* 2018;11:1345.
17. Van Den Bulcke AI, Bogdanov B, De Rooze N, Schacht EH, Cornelissen M. BerghmansH. Structural and rheological properties of methacrylamide modified gelatin hydrogels. *Biomacromolecules* 2000;1:131—8.
18. Yue K, Trujillo-de Santiago G, Alvarez MM, Tamayol A, Annabi N, Khademhosseini A. Synthesis, properties, and biomedical applications of gelatin methacryloyl (GelMA) hydrogels. *Biomaterials* 2015;73:254—71.
19. Zhu Y, Yu X, Liu H, et al. Strategies of functionalized GelMA-based bioinks for bone regeneration: recent advances and future perspectives. *Bioact Mater* 2024;38:346—73.
20. Farshidfar N, Iravani S, Varma RS. Alginate-based biomaterials in tissue engineering and regenerative medicine. *Mar Drugs* 2023;21:189.
21. Yang M, Zhang ZC, Liu Y, et al. Function and mechanism of RGD in bone and cartilage tissue engineering. *Front Bioeng Biotechnol* 2021;9:773636.
22. Kumar VB, Tiwari OS, Finkelstein-Zuta G, Rencus-Lazar S, Gazit E. Design of functional RGD peptide-based biomaterials for tissue engineering. *Pharmaceutics* 2023;15:345.
23. Ansari S, Pouraghaei Sevari S, Chen C, Sarrion P, Moshaverinia A. RGD-modified alginate—GelMA hydrogel sheet containing gingival mesenchymal stem cells: a unique platform for wound healing and soft tissue regeneration. *ACS Biomater Sci Eng* 2021;7:3774—82.
24. Łabowska MB, Cierluk K, Jankowska AM, Kulbacka J, Detyna J, Michalak I. A review on the adaption of alginate-gelatin hydrogels for 3D cultures and bioprinting. *Materials (Basel)* 2021;14:858.
25. Annabi N, Nichol JW, Zhong X, et al. Controlling the porosity and microarchitecture of hydrogels for tissue engineering. *Tissue Eng Part B Rev* 2010;16:371—83.
26. Derkach SR, Voron'ko NG, Sokolan NI, Kolotova DS, Kuchina YA. Interactions between gelatin and sodium alginate: UV and FTIR studies. *J Dispersion Sci Technol* 2019;41:690—8.
27. Paglia EB, de Freitas GP, Baldin EKK, Pacheco JEC, Carvalho HF, Beppu MM. Innovative approaches in alginate grafting: amino acids of RGD peptide composition for biomimetic and biocompatible biomaterial. *Int J Biol Macromol* 2025;322:147080.
28. Sauce-Guevara MA, García-Schejtman SD, Alarcon EI, Bernal-Chavez SA, Mendez-Rojas MA. Development and characterization of an injectable alginate/chitosan composite hydrogel reinforced with cyclic-RGD functionalized graphene oxide for potential tissue regeneration applications. *Pharmaceuticals (Basel)* 2025;18:616.
29. Cao Y, Liu C, Ye W, Zhao T, Fu F. Functional hydrogel interfaces for cartilage and bone regeneration. *Adv Healthcare Mater* 2025;14:2403079.
30. Beamish JA, Fu AY, Choi AJ, Haq NA, Kottke-Marchant K, Marchant RE. The influence of RGD-bearing hydrogels on the re-expression of contractile vascular smooth muscle cell phenotype. *Biomaterials* 2009;30:4127—35.
31. Chu C, Schmidt JJ, Carnes K, Zhang Z, Kong HJ, Hofmann MC. Three-dimensional synthetic niche components to control germ cell proliferation. *Tissue Eng* 2009;15:255—62.
32. He X, Ma J, Jabbari E. Effect of grafting RGD and BMP-2 protein-derived peptides to a hydrogel substrate on osteogenic differentiation of marrow stromal cells. *Langmuir* 2008;24:12508—16.
33. Moore NM, Lin NJ, Gallant ND, Becker ML. Synergistic enhancement of human bone marrow stromal cell proliferation and osteogenic differentiation on BMP-2-derived and RGD peptide concentration gradients. *Acta Biomater* 2011;7:2091—100.
34. Bellis SL. Advantages of RGD peptides for directing cell association with biomaterials. *Biomaterials* 2011;32:4205—10.